

Craig M Brown

List of Publications by Year in descending order

Source: [//exaly.com/author-pdf/7007231/publications.pdf](https://exaly.com/author-pdf/7007231/publications.pdf)

Version: 2024-02-01

217
papers

19,285
citations

19477

61
h-index

12194

135
g-index

234
all docs

234
docs citations

234
times ranked

21427
citing authors

#	ARTICLE	IF	CITATIONS
1	Small-pore hydridic frameworks store densely packed hydrogen. <i>Nature Chemistry</i> , 2024, 16, 809-816.	14.3	4
2	Water-enhanced CO ₂ capture with molecular salt sodium guanidinate. <i>Journal of Materials Chemistry A</i> , 2024, 12, 16748-16759.	10.5	0
3	Measuring the Influence of CO ₂ and Water Vapor on the Dynamics in Polyethylenimine To Understand the Direct Air Capture of CO ₂ from the Environment. <i>Chemistry of Materials</i> , 2024, 36, 6130-6143.	7.1	0
4	Neutron Vibrational Spectroscopic Study of the Acetylene: Ammonia (1:1) Cocrystal Relevant to Titan, Saturn's Moon. <i>Journal of Physical Chemistry A</i> , 2024, 128, 5676-5683.	2.6	1
5	The Influence of Reorientational and Vibrational Dynamics on the Mg ²⁺ Conductivity in Mg(BH ₄) ₂ ·CH ₃ NH ₂ . <i>Chemistry of Materials</i> , 2024, 36, 9784-9792.	7.1	0
6	Neutron scattering studies of materials for hydrogen storage. , 2023, , 3-50.		6
7	Flexing of a Metal-Organic Framework upon Hydrocarbon Adsorption: Atomic Level Insights from Neutron Scattering. <i>Chemistry of Materials</i> , 2023, 35, 1387-1394.	7.1	6
8	Multivariate Flexible Framework with High Usable Hydrogen Capacity in a Reduced Pressure Swing Process. <i>Journal of the American Chemical Society</i> , 2023, 145, 8033-8042.	14.6	11
9	Noncryogenic Air Separation Using Aluminum Formate Al(HCOO) ₃ (ALF). <i>Journal of the American Chemical Society</i> , 2023, 145, 9850-9856.	14.6	14
10	Quantum disordered ground state in the triangular-lattice magnet NaRuO ₂ . <i>Nature Physics</i> , 2023, 19, 943-949.	11.8	17
11	Exclusive Recognition of CO ₂ from Hydrocarbons by Aluminum Formate with Hydrogen-Confined Pore Cavities. <i>Journal of the American Chemical Society</i> , 2023, 145, 11643-11649.	14.6	25
12	Adaptive Pore Opening to Form Tailored Adsorption Sites in a Cooperatively Flexible Framework Enables Record Inverse Propane/Propylene Separation. <i>Journal of the American Chemical Society</i> , 2023, 145, 21955-21965.	14.6	7
13	Hydrogen Storage with Aluminum Formate, ALF: Experimental, Computational, and Technoeconomic Studies. <i>Journal of the American Chemical Society</i> , 2023, 145, 22150-22157.	14.6	6
14	Investigating the non-classical M-H ₂ bonding in OsClH ₃ (PPh ₃) ₃ . <i>Journal of Alloys and Compounds</i> , 2022, 894, 162445.	5.7	1
15	Neutron Vibrational Spectroscopic Evidence for Short H···H Contacts in the <i>R</i> NiInH _{1.4;1.6} (<i>R</i> = Ce, La) Metal Hydride. <i>Neutron News</i> , 2022, 33, 7-9.	0.2	1
16	Stacking Faults Assist Lithium-Ion Conduction in a Halide-Based Superionic Conductor. <i>Journal of the American Chemical Society</i> , 2022, 144, 5795-5811.	14.6	66
17	Magnetic-Field-Induced Dielectric Anomalies in Cobalt-Containing Garnets. <i>Inorganic Chemistry</i> , 2022, 61, 5452-5458.	4.2	0
18	Lattice Dynamics in the NASICON NaZr ₂ (PO ₄) ₃ Solid Electrolyte from Temperature-Dependent Neutron Diffraction, NMR, and Ab Initio Computational Studies. <i>Chemistry of Materials</i> , 2022, 34, 4029-4038.	7.1	8

#	ARTICLE	IF	CITATIONS
19	Turning Molecular Springs into Nano-Shock Absorbers: The Effect of Macroscopic Morphology and Crystal Size on the Dynamic Hysteresis of Water Intrusion/Extrusion into/from Hydrophobic Nanopores. ACS Applied Materials & Interfaces, 2022, 14, 26699-26713.	8.3	13
20	Polyoxocationic antimony oxide cluster with acidic protons. Science Advances, 2022, 8, .	10.9	5
21	Bi ₁₂ O ₁₇ Cl ₂ with a Sextuple Bi ³⁺ O Layer Composed of Rock-Salt and Fluorite Units and its Structural Conversion through Fluorination to Enhance Photocatalytic Activity. Advanced Functional Materials, 2022, 32, .	16.5	18
22	Influence of Inorganic Layer Thickness on Methylammonium Dynamics in Hybrid Perovskite Derivatives. Chemistry of Materials, 2022, 34, 8316-8323.	7.1	7
23	Aluminum formate, Al(HCOO) ₃ : An earth-abundant, scalable, and highly selective material for CO ₂ capture. Science Advances, 2022, 8, .	10.9	51
24	Ambient-Temperature Hydrogen Storage via Vanadium(II)-Dihydrogen Complexation in a Metal-Organic Framework. Journal of the American Chemical Society, 2021, 143, 6248-6256.	14.6	105
25	Compact Thermal Actuation by Water and Flexible Hydrophobic Nanopore. ACS Nano, 2021, 15, 9048-9056.	15.3	14
26	Spin Frustration in Double Perovskite Oxides and Oxynitrides: Enhanced Frustration in La ₂ MnTaO ₅ N with a Large Octahedral Rotation. Inorganic Chemistry, 2021, 60, 8252-8258.	4.2	9
27	Antiferromagnetic Order and Spin-Canting Transition in the Corrugated Square Net Compound Cu ₃ (TeO ₄)(SO ₄) \cdot H ₂ O. Inorganic Chemistry, 2021, 60, 10565-10571.	4.2	4
28	Magnetic structure, excitations and short-range order in honeycomb Na ₂ Ni ₂ TeO ₆ . Journal of Physics Condensed Matter, 2021, 33, 375803.	1.9	3
29	Spin Reorientation in Antiferromagnetic Layered FePt ₅ P. ACS Applied Electronic Materials, 2021, 3, 3501-3508.	4.4	9
30	Enhanced Magnetic Interaction by Face-Shared Hydride Anions in 6H-BaCrO ₂ H. Inorganic Chemistry, 2021, 60, 11957-11963.	4.2	14
31	Observation of an Intermediate to H ₂ Binding in a Metal-Organic Framework. Journal of the American Chemical Society, 2021, 143, 14884-14894.	14.6	42
32	The Rietveld Refinement Method: Half of a Century Anniversary. Crystal Growth and Design, 2021, 21, 4821-4822.	3.2	16
33	Magnetic properties and signatures of moment ordering in the triangular lattice antiferromagnet $\langle \text{mml:math} \text{xmlns:mml="http://www.w3.org/1998/Math/MathML"} \rangle \langle \text{mml:msub} \rangle \langle \text{mml:mi} \rangle \text{KCeO} \langle \text{mml:mi} \rangle \langle \text{mml:mn} \rangle 2 \langle \text{mml:mn} \rangle \langle \text{mml:msub} \rangle \langle \text{mml:mi} \rangle \text{Physical Review B, 2021, 104, .}$	3.3	10
34	Conduction Band Control of Oxyhalides with a Triple-Fluorite Layer for Visible Light Photocatalysis. Journal of the American Chemical Society, 2021, 143, 2491-2499.	14.6	63
35	Chemical Bonding Governs Complex Magnetism in MnPt ₅ P. Inorganic Chemistry, 2021, 60, 87-96.	4.2	10
36	Iridate Li ₈ IrO ₆ : An Antiferromagnetic Insulator. Inorganic Chemistry, 2021, 60, 17201-17211.	4.2	2

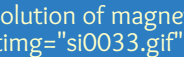
#	ARTICLE	IF	CITATIONS
37	Structural resolution and mechanistic insight into hydrogen adsorption in flexible ZIF-7. <i>Chemical Science</i> , 2021, 12, 15620-15631.	7.8	23
38	Physical properties of the quasi-two-dimensional square lattice antiferromagnet BaMn_2O_7 . <i>Physical Review B</i> , 2021, 104, .	3.3	12
39	Efficient and tunable one-dimensional charge transport in layered lanthanide metal-organic frameworks. <i>Nature Chemistry</i> , 2020, 12, 131-136.	14.3	232
40	Strain-induced creation and switching of anion vacancy layers in perovskite oxynitrides. <i>Nature Communications</i> , 2020, 11, 5923.	13.2	26
41	Elucidating the Structure of the Metal-Organic Framework Ru-HKUST-1. <i>Chemistry of Materials</i> , 2020, 32, 7710-7715.	7.1	9
42	Dynamics of Hydroxyl Anions Promotes Lithium Ion Conduction in Antiperovskite Li_2OHCl . <i>Chemistry of Materials</i> , 2020, 32, 8481-8491.	7.1	57
43	Peritectic phase transition of benzene and acetonitrile into a cocrystal relevant to Titan, Saturn's moon. <i>Chemical Communications</i> , 2020, 56, 13520-13523.	4.2	13
44	Self-adjusting binding pockets enhance H_2 and CH_4 adsorption in a uranium-based metal-organic framework. <i>Chemical Science</i> , 2020, 11, 6709-6716.	7.8	25
45	Special section "Crystallography and properties of metal-organic framework (MOF) compounds. <i>Powder Diffraction</i> , 2020, 35, 2-2.	0.3	0
46	Negative cooperativity upon hydrogen bond-stabilized O_2 adsorption in a redox-active metal-organic framework. <i>Nature Communications</i> , 2020, 11, 3087.	13.2	45
47	Inter-Kramers Transitions and Spin-Phonon Couplings in a Lanthanide-Based Single-Molecule Magnet. <i>Inorganic Chemistry</i> , 2020, 59, 5218-5230.	4.2	26
48	Metastability and Reversibility of Anionic Redox-Based Cathode for High-Energy Rechargeable Batteries. <i>Cell Reports Physical Science</i> , 2020, 1, 100028.	5.8	41
49	Molecular Insight into Fluorocarbon Adsorption in Pore Expanded Metal-Organic Framework Analogs. <i>Journal of the American Chemical Society</i> , 2020, 142, 3002-3012.	14.6	48
50	Understanding How Ligand Functionalization Influences CO_2 and N_2 Adsorption in a Sodalite Metal-Organic Framework. <i>Chemistry of Materials</i> , 2020, 32, 1526-1536.	7.1	19
51	Neutron diffraction structural study of CO_2 binding in mixed-metal CPM-200 metal-organic frameworks. <i>Chemical Communications</i> , 2020, 56, 2574-2577.	4.2	5
52	Certification of Standard Reference Material 660c for powder diffraction. <i>Powder Diffraction</i> , 2020, 35, 17-22.	0.3	19
53	Competing antiferromagnetic-ferromagnetic states in a Kitaev honeycomb magnet. <i>Physical Review B</i> , 2020, 102, .	3.1	4
54	Long-range magnetic order in hydroxide-layer-doped $(\text{Li}_{1-x}\text{Fe}_x\text{MnyOD})\text{FeSe}$. <i>Physical Review Materials</i> , 2020, 4, .	2.5	3

#	ARTICLE	IF	CITATIONS
55	Accessing New Charge-Transfer Complexes by Mechanochemistry: A Tetrathiafulvalene Chloranilic Acid Polymorph Containing Segregated Tetrathiafulvalene Stacks. <i>Crystal Growth and Design</i> , 2019, 19, 4970-4980.	3.2	6
56	Field-tunable quantum disordered ground state in the triangular-lattice antiferromagnet NaYbO ₂ . <i>Nature Physics</i> , 2019, 15, 1058-1064.	11.8	155
57	Dynamical Phase Transitions and Cation Orientation-Dependent Photoconductivity in CH(NH ₂) ₂ PbBr ₃ . , 2019, 1, 260-264.		38
58	Understanding Gas Storage in Cuboctahedral Porous Coordination Cages. <i>Journal of the American Chemical Society</i> , 2019, 141, 12128-12138.	14.6	81
59	Realization of interlayer ferromagnetic interaction in $MnS_{2-x}T_x$ toward the magnetic Weyl semimetal state. <i>Physical Review B</i> , 2019, 100, .	3.3	87
60	Elusive Valence Transition in Mixed-Valence Sesquioxide Cs ₄ O ₆ . <i>Inorganic Chemistry</i> , 2019, 58, 14532-14541.	4.2	6
61	Correction to Dynamical Phase Transitions and Cation Orientation-Dependent Photoconductivity in CH(NH ₂) ₂ PbBr ₃ . , 2019, 1, 481-481.		0
62	Competing Polar and Antipolar Structures in the Ruddlesden-Popper Layered Perovskite Li ₂ SrNb ₂ O ₇ . <i>Chemistry of Materials</i> , 2019, 31, 4418-4425.	7.1	31
63	High-Pressure Synthesis of Non-Stoichiometric Li _x WO ₃ (0.5 ≤ x ≤ 1.0) with LiNbO ₃ Structure. <i>Inorganics</i> , 2019, 7, 63.	2.8	9
64	Rattling Behavior in a Simple Perovskite NaWO ₃ . <i>Inorganic Chemistry</i> , 2019, 58, 6790-6795.	4.2	10
65	Special section: crystallography and properties of metal organic framework (MOF) compounds. <i>Powder Diffraction</i> , 2019, 34, 2-2.	0.3	0
66	New insights into water dynamics of Portland cement paste with nano-additives using quasielastic neutron scattering. <i>Journal of Materials Science</i> , 2019, 54, 4710-4718.	3.7	4
67	Neutron Instruments for Research in Coordination Chemistry. <i>European Journal of Inorganic Chemistry</i> , 2019, 2019, 1065-1089.	2.2	29
68	High-Pressure Synthesis of A ₂ NiO ₂ Ag ₂ Se ₂ (A=Sr, Ba) with a High-Spin Ni ²⁺ in Square-Planar Coordination. <i>Angewandte Chemie - International Edition</i> , 2019, 58, 756-759.	14.8	27
69	Probing Magnetic Excitations in Co ^{II} Single-Molecule Magnets by Inelastic Neutron Scattering. <i>European Journal of Inorganic Chemistry</i> , 2019, 2019, 1119-1127.	2.2	15
70	An <i>In Situ</i> Neutron Diffraction and DFT Study of Hydrogen Adsorption in a Sodalite-Type Metal-Organic Framework, Cu ^{II} Tri. <i>European Journal of Inorganic Chemistry</i> , 2019, 2019, 1147-1154.	2.2	16
71	Deciphering structural and magnetic disorder in the chiral skyrmion host materials $Co_{1-x}Mn_x$		

#	ARTICLE	IF	CITATIONS
73	In situ powder X-ray crystallography for gas sorption in metal-organic frameworks. Acta Crystallographica Section A: Foundations and Advances, 2019, 75, a298-a298.	0.1	0
74	Rapid Microwave Preparation and Composition Tuning of the High-Performance Magnetocalorics (Mn,Fe) ₂ (P,Si). ACS Applied Materials & Interfaces, 2018, 10, 7208-7213.	8.3	19
75	An experimental and computational study of CO ₂ adsorption in the sodalite-type M-BTT (M) Tj ETQq1 1 0.784314 rgBT / 0.4579-4588.	7.8	47
76	Magnetic ordering in a frustrated bow-tie lattice. Journal of Materials Chemistry C, 2018, 6, 4541-4548.	5.6	5
77	Separation of Xylene Isomers through Multiple Metal Site Interactions in Metal-Organic Frameworks. Journal of the American Chemical Society, 2018, 140, 3412-3422.	14.6	162
78	Selective Hydride Occupation in BaVO ₃ H _x (0.3 ≤ x ≤ 0.8) with Face- and Corner-Shared Octahedra. Chemistry of Materials, 2018, 30, 1566-1574.	7.1	26
79	Unravelling Solid-State Redox Chemistry in Li _{1.3} Nb _{0.3} Mn _{0.4} O ₂ Single-Crystal Cathode Material. Chemistry of Materials, 2018, 30, 1655-1666.	7.1	87
80	H ₂ Adsorption on Cu(I)-SSZ-13. Journal of Physical Chemistry C, 2018, 122, 540-548.	3.3	17
81	Proton and ammonia intercalation into layered iron chalcogenides. Chemical Communications, 2018, 54, 6895-6898.	4.2	5
82	Quantum Dynamics of H_2 Trapped within Organic Clathrate Cages. Physical Review Letters, 2018, 120, 120402.	8.0	7
83	Imaging appearance of fibrosing diseases of the retroperitoneum: can a definitive diagnosis be made?. Abdominal Radiology, 2018, 43, 1204-1214.	2.2	13
84	Record High Hydrogen Storage Capacity in the Metal-Organic Framework Ni ₂ (m-dobdc) at Near-Ambient Temperatures. Chemistry of Materials, 2018, 30, 8179-8189.	7.1	200
85	Defect-driven extreme magnetoresistance in an I-Mn-V semiconductor. Applied Physics Letters, 2018, 113, .	3.2	6
86	Certification of Standard Reference Material 1879b respirable cristobalite. Powder Diffraction, 2018, 33, 202-208.	0.3	1
87	Gas adsorption in an isostructural series of pillared coordination cages. Chemical Communications, 2018, 54, 6392-6395.	4.2	19
88	Spin-phonon couplings in transition metal complexes with slow magnetic relaxation. Nature Communications, 2018, 9, 2572.	13.2	99
89	Methane Storage in Paddlewheel-Based Porous Coordination Cages. Journal of the American Chemical Society, 2018, 140, 11153-11157.	14.6	89
90	On the Structure-Property Relationships of Cation-Exchanged ZK5 Zeolites for CO ₂ Adsorption. ChemSusChem, 2017, 10, 946-957.	7.5	38

#	ARTICLE	IF	CITATIONS
91	Performance of van der Waals Corrected Functionals for Guest Adsorption in the Metal-Organic Frameworks. <i>Journal of Physical Chemistry A</i> , 2017, 121, 4139-4151.	2.6	49
92	Formation of [Cu ₂ O] ²⁺ and [Cu ₂ O] ²⁺ toward C-H Bond Activation in Cu-SSZ-13 and Cu-SSZ-39. <i>ACS Catalysis</i> , 2017, 7, 4291-4303.	11.7	207
93	Metal-insulator transition tuned by magnetic field in Bi _{1.7} V ₈ O ₁₆ hollandite. <i>Journal of Materials Chemistry C</i> , 2017, 5, 4967-4976.	5.6	2
94	Reversible Capture and Release of Cl ₂ and Br ₂ with a Redox-Active Metal-Organic Framework. <i>Journal of the American Chemical Society</i> , 2017, 139, 5992-5997.	14.6	105
95	Selective Gas Adsorption in Highly Porous Chromium(II)-Based Metal-Organic Polyhedra. <i>Chemistry of Materials</i> , 2017, 29, 8583-8587.	7.1	74
96	Electronic Conductivity in a Porous Vanadyl Prussian Blue Analogue upon Air Exposure. <i>Inorganic Chemistry</i> , 2017, 56, 12682-12686.	4.2	13
97	Ising-like antiferromagnetism on the octahedral sublattice of a cobalt-containing garnet and the potential for quantum criticality. <i>Physical Review B</i> , 2017, 95, .	3.3	8
98	Combining microscopic and macroscopic probes to untangle the single-ion anisotropy and exchange energies in an S ₁ quantum antiferromagnet. <i>Physical Review B</i> , 2017, 95, .	3.3	15
99	Cubic lead perovskite PbMoO ₃ with anomalous metallic behavior. <i>Physical Review B</i> , 2017, 95, .	3.3	14
100	Origin of long lifetime of band-edge charge carriers in organic-inorganic lead iodide perovskites. <i>Proceedings of the National Academy of Sciences of the United States of America</i> , 2017, 114, 7519-7524.	7.6	149
101	Pressure tuning of collapse of helimagnetic structure in Au ₂ Cr ₂ Sn ₂ . <i>Physical Review B</i> , 2017, 96, .	3.3	2
102	Hydrogen Storage and Selective, Reversible O ₂ Adsorption in a Metal-Organic Framework with Open Chromium(II) Sites. <i>Angewandte Chemie - International Edition</i> , 2016, 55, 8605-8609.	14.8	107
103	Hydrogen Storage and Selective, Reversible O ₂ Adsorption in a Metal-Organic Framework with Open Chromium(II) Sites. <i>Angewandte Chemie</i> , 2016, 128, 8747-8751.	2.1	24
104	Metastable Layered Cobalt Chalcogenides from Topochemical Deintercalation. <i>Journal of the American Chemical Society</i> , 2016, 138, 16432-16442.	14.6	64
105	Quasi-Elastic Neutron Scattering Studies of Hydrogen Dynamics for Nanoconfined NaAlH ₄ . <i>Journal of Physical Chemistry C</i> , 2016, 120, 14863-14873.	3.3	9
106	The magnetic transitions and dynamics in the multiferroic Lu _{0.5} Sc _{0.5} FeO ₃ . <i>MRS Advances</i> , 2016, 1, 565-571.	1.0	4
107	High Thermopower with Metallic Conductivity in p-Type Li-Substituted PbPdO ₂ . <i>Chemistry of Materials</i> , 2016, 28, 3367-3373.	7.1	26
108	The low-temperature structural behavior of sodium 1-carba-closo-decaborate: NaCB ₉ H ₁₀ . <i>Journal of Solid State Chemistry</i> , 2016, 243, 162-167.	3.0	13

#	ARTICLE	IF	CITATIONS
109	ZnTaO ₂ N: Stabilized High-Temperature LiNbO ₃ -type Structure. Journal of the American Chemical Society, 2016, 138, 15950-15955.	14.6	26
110	High-Pressure Synthesis of Manganese Oxyhydride with Partial Anion Order. Angewandte Chemie - International Edition, 2016, 55, 9667-9670.	14.8	31
111	Local Jahn-Teller distortions and orbital ordering in Ba ₃ Cu _{1+x} Sb ₂ xO ₉ investigated by neutron scattering. Physical Review B, 2016, 93, .	3.3	4
112	Hydration-induced spin-glass state in a frustrated Na-Mn-O triangular lattice. Physical Review B, 2016, 93, .	3.3	13
113	Entropy-driven structural transition and kinetic trapping in formamidinium lead iodide perovskite. Science Advances, 2016, 2, e1601650.	10.9	219
114	Three-dimensional protonic conductivity in porous organic cage solids. Nature Communications, 2016, 7, 12750.	13.2	137
115	Tuning the Adsorption-Induced Phase Change in the Flexible Metal-Organic Framework Co(bdp). Journal of the American Chemical Society, 2016, 138, 15019-15026.	14.6	127
116	Adsorption of two gas molecules at a single metal site in a metal-organic framework. Chemical Communications, 2016, 52, 8251-8254.	4.2	47
117	Water dynamics in cement paste at early age prepared with pozzolanic volcanic ash and Ordinary Portland Cement using quasielastic neutron scattering. Cement and Concrete Research, 2016, 86, 55-62.	11.1	30
118	Dynamics of Pyramidal SiH ₃ ⁺ Ions in ASiH ₃ (A = K and Rb) Investigated with Quasielastic Neutron Scattering. Journal of Physical Chemistry C, 2016, 120, 6369-6376.	3.3	17
119	Improved Catalytic Activity and Stability of a Palladium Pincer Complex by Incorporation into a Metal-Organic Framework. Journal of the American Chemical Society, 2016, 138, 1780-1783.	14.6	146
120	Topochemical Nitridation with Anion Vacancy-Assisted N ³⁺ /O ²⁺ Exchange. Journal of the American Chemical Society, 2016, 138, 3211-3217.	14.6	47
121	Hydrogen Storage in the Expanded Pore Metal-Organic Frameworks M ₂ (dobpc) (M = Mg, Tj) $\frac{1}{7.1} \frac{0.784314}{180} \text{ rgB}$		
122	MnTaO ₂ N: Polar LiNbO ₃ -type Oxynitride with a Helical Spin Order. Angewandte Chemie - International Edition, 2015, 54, 516-521.	14.8	44
123	Understanding Small-Molecule Interactions in Metal-Organic Frameworks: Coupling Experiment with Theory. Advanced Materials, 2015, 27, 5785-5796.	24.3	35
124	MnTaO ₂ N: Polar LiNbO ₃ -type Oxynitride with a Helical Spin Order. Angewandte Chemie, 2015, 127, 526-531.	2.1	10
125	Oxygen interstitials and vacancies in LaSrGa ₃ O ₇ -based melilites. Journal of Solid State Chemistry, 2015, 230, 309-317.	3.0	20
126	Magnetic Structure and Exchange Interactions in Quasi-One-Dimensional MnCl ₂ (urea) ₂ . Inorganic Chemistry, 2015, 54, 11897-11905.	4.2	20

#	ARTICLE	IF	CITATIONS
127	Inducing Ferrimagnetism in Insulating Hollandite Ba _{1.2} Mn ₈ O ₁₆ . Chemistry of Materials, 2015, 27, 515-525.	7.1	22
128	Gradual Release of Strongly Bound Nitric Oxide from Fe ₂ (NO) ₂ (dobdc). Journal of the American Chemical Society, 2015, 137, 3466-3469.	14.6	84
129	Flexible metal-organic framework compounds: In situ studies for selective CO ₂ capture. Journal of Alloys and Compounds, 2015, 647, 24-34.	5.7	25
130	Stabilization of cubic Sr ₂ FeMoO ₆ through topochemical reduction. Chemical Communications, 2015, 51, 12201-12204.	4.2	9
131	Methane storage in flexible metal-organic frameworks with intrinsic thermal management. Nature, 2015, 527, 357-361.	36.2	865
132	Rotational dynamics of organic cations in the CH ₃ NH ₃ PbI ₃ perovskite. Physical Chemistry Chemical Physics, 2015, 17, 31278-31286.	2.9	222
133	A labile hydride strategy for the synthesis of heavily nitrized BaTiO ₃ . Nature Chemistry, 2015, 7, 1017-1023.	14.3	119
134	Critical Factors Driving the High Volumetric Uptake of Methane in Cu ₃ (btc) ₂ . Journal of the American Chemical Society, 2015, 137, 10816-10825.	14.6	74
135	Evolution of magnetism in the 		

#	ARTICLE	IF	CITATIONS
145	M ₂ (dobdc) (M = Mg, Mn, Fe, Co, Ni) Metal-Organic Frameworks Exhibiting Increased Charge Density and Enhanced H ₂ Binding at the Open Metal Sites. <i>Journal of the American Chemical Society</i> , 2014, 136, 12119-12129.	14.6	220
146	Surface compression of light adsorbates inside microporous PFA-derived carbons. <i>Carbon</i> , 2013, 60, 538-549.	10.7	34
147	Evaluation of cation-exchanged zeolite adsorbents for post-combustion carbon dioxide capture. <i>Energy and Environmental Science</i> , 2013, 6, 128-138.	32.2	343
148	Chemical spectroscopy using neutrons. <i>Chemical Physics</i> , 2013, 427, 1-2.	2.0	2
149	Structure and spectroscopy of hydrogen adsorbed in a nickel metal-organic framework. <i>Chemical Physics</i> , 2013, 427, 3-8.	2.0	23
150	Selective adsorption of ethylene over ethane and propylene over propane in the metal-organic frameworks M ₂ (dobdc) (M = Mg, Mn, Fe, Co, Ni, Zn). <i>Chemical Science</i> , 2013, 4, 2054.	7.8	409
151	Mn(dca) ₂ (o-phen) {dca=dicyanamide; o-phen=1,10-phenanthroline}: Long-range magnetic order in a low-dimensional Mn-dca polymer. <i>Polyhedron</i> , 2013, 52, 679-688.	2.3	9
152	Noble Gas Adsorption in Copper Trimesate, HKUST-1: An Experimental and Computational Study. <i>Journal of Physical Chemistry C</i> , 2013, 117, 20116-20126.	3.3	93
153	Hydrogen diffusion in potassium intercalated graphite studied by quasielastic neutron scattering. <i>Journal of Chemical Physics</i> , 2012, 137, 224704.	3.1	5
154	Unconventional, Highly Selective CO ₂ Adsorption in Zeolite SSZ-13. <i>Journal of the American Chemical Society</i> , 2012, 134, 1970-1973.	14.6	372
155	Hydrogen adsorption in the metal-organic frameworks Fe ₂ (dobdc) and Fe ₂ (O ₂)(dobdc). <i>Dalton Transactions</i> , 2012, 41, 4180.	3.4	78
156	Spectroscopic Identification of Hydrogen Spillover Species in Ruthenium-Modified High Surface Area Carbons by Diffuse Reflectance Infrared Fourier Transform Spectroscopy. <i>Journal of Physical Chemistry C</i> , 2012, 116, 26744-26755.	3.3	32
157	Metal-assisted hydrogen storage on Pt-decorated single-walled carbon nanohorns. <i>Carbon</i> , 2012, 50, 4953-4964.	10.7	69
158	Redox-Promoting Protein Motions in Rubredoxin. <i>Journal of Physical Chemistry B</i> , 2011, 115, 8925-8936.	2.7	15
159	Structural Study of D ₂ within the Trimodal Pore System of a Metal Organic Framework. <i>Journal of Physical Chemistry C</i> , 2011, 115, 8851-8857.	3.3	34
160	Site-Specific CO ₂ Adsorption and Zero Thermal Expansion in an Anisotropic Pore Network. <i>Journal of Physical Chemistry C</i> , 2011, 115, 24915-24919.	3.3	144
161	Neutron Scattering and Spectroscopic Studies of Hydrogen Adsorption in Cr ₃ (BTC) ₂ —A Metal-Organic Framework with Exposed Cr ²⁺ Sites. <i>Journal of Physical Chemistry C</i> , 2011, 115, 8414-8421.	3.3	51
162	Hydrogen storage properties and neutron scattering studies of Mg ₂ (dobdc)—a metal-organic framework with open Mg ²⁺ adsorption sites. <i>Chemical Communications</i> , 2011, 47, 1157-1159.	4.2	182

#	ARTICLE	IF	CITATIONS
163	Selective Binding of O ₂ over N ₂ in a Redox-Active Metal-Organic Framework with Open Iron(II) Coordination Sites. <i>Journal of the American Chemical Society</i> , 2011, 133, 14814-14822.	14.6	486
164	Micro-channel development and hydrogen adsorption properties in templated microporous carbons containing platinum nanoparticles. <i>Carbon</i> , 2011, 49, 1305-1317.	10.7	31
165	Hydrogen storage and carbon dioxide capture in an iron-based sodalite-type metal-organic framework (Fe-BTT) discovered via high-throughput methods. <i>Chemical Science</i> , 2010, 1, 184.	7.8	300
166	Identifying the Specific Nanostructures Responsible for the High Thermoelectric Performance of (Bi,Sb) ₂ Te ₃ Nanocomposites. <i>Nano Letters</i> , 2010, 10, 3283-3289.	9.5	493
167	Metal-Organic Frameworks with Exceptionally High Methane Uptake: Where and How is Methane Stored?. <i>Chemistry - A European Journal</i> , 2010, 16, 5205-5214.	3.9	233
168	Highly-Selective and Reversible O ₂ Binding in Cr ₃ (1,3,5-benzenetricarboxylate) ₂ . <i>Journal of the American Chemical Society</i> , 2010, 132, 7856-7857.	14.6	311
169	User Facilities: The Education of New Neutron Users. <i>AIP Conference Proceedings</i> , 2009, , .	1.0	1
170	Hydrogen adsorption in HKUST-1: a combined inelastic neutron scattering and first-principles study. <i>Nanotechnology</i> , 2009, 20, 204025.	2.7	113
171	Detection of Hydrogen Spillover in Palladium-Modified Activated Carbon Fibers during Hydrogen Adsorption. <i>Journal of Physical Chemistry C</i> , 2009, 113, 5886-5890.	3.3	154
172	Role of Cation Size on the Structural Behavior of the Alkali-Metal Dodecahydro-closo-Dodecaborates. <i>Journal of Physical Chemistry C</i> , 2009, 113, 11187-11189.	3.3	58
173	High Capacity Hydrogen Adsorption in Cu(II) Tetracarboxylate Framework Materials: The Role of Pore Size, Ligand Functionalization, and Exposed Metal Sites. <i>Journal of the American Chemical Society</i> , 2009, 131, 2159-2171.	14.6	726
174	Neutron powder diffraction of metal-organic frameworks for hydrogen storage. <i>Pramana - Journal of Physics</i> , 2008, 71, 755-760.	1.8	18
175	The design of a bismuth-based auxiliary filter for the removal of spurious background scattering associated with filter-analyzer neutron spectrometers. <i>Nuclear Instruments and Methods in Physics Research, Section A: Accelerators, Spectrometers, Detectors and Associated Equipment</i> , 2008, 588, 406-413.	1.6	69
176	Quasielastic neutron scattering of ¹⁵ NH ₃ and ¹⁰ BH ₃ rotational dynamics in orthorhombic ammonia borane. <i>Chemical Physics Letters</i> , 2008, 459, 85-88.	2.7	27
177	Reversible Structural Transition in MIL-53 with Large Temperature Hysteresis. <i>Journal of the American Chemical Society</i> , 2008, 130, 11813-11818.	14.6	408
178	Hydrogen Adsorption in a Highly Stable Porous Rare-Earth Metal-Organic Framework: Sorption Properties and Neutron Diffraction Studies. <i>Journal of the American Chemical Society</i> , 2008, 130, 9626-9627.	14.6	294
179	Inelastic neutron scattering from confined molecular oxygen. <i>Physical Review B</i> , 2008, 78, .	3.3	10
180	Increasing the Density of Adsorbed Hydrogen with Coordinatively Unsaturated Metal Centers in Metal-Organic Frameworks. <i>Langmuir</i> , 2008, 24, 4772-4777.	3.7	261

#	ARTICLE	IF	CITATIONS
181	Inelastic neutron scattering study of hydrogen in d8-THF·D2O ice clathrate. <i>Journal of Chemical Physics</i> , 2007, 127, 134505.	3.1	32
182	Structural Characterization of D ₂ in Cu ₃ (1,3,5-Benzenetricarboxylate) ₂ Using Neutron Powder Diffraction. <i>Materials Science Forum</i> , 2007, 561-565, 1601-1604.	0.2	2
183	Hydrogen Adsorption in MOF-74 Studied by Inelastic Neutron Scattering. <i>Materials Research Society Symposia Proceedings</i> , 2007, 1041, 1.	0.1	1
184	Neutron vibrational spectroscopy of the Pr ₂ Fe ₁₇ -based hydrides. <i>Journal of Alloys and Compounds</i> , 2007, 446-447, 504-507.	5.7	6
185	Inelastic neutron scattering of H ₂ adsorbed in HKUST-1. <i>Journal of Alloys and Compounds</i> , 2007, 446-447, 385-388.	5.7	74
186	Inelastic neutron scattering of H ₂ adsorbed on boron substituted single walled carbon nanotubes. <i>Journal of Alloys and Compounds</i> , 2007, 446-447, 368-372.	5.7	16
187	Observation of Cu ₂ +H ₂ Interactions in a Fully Desolvated Sodalite-Type Metal-Organic Framework. <i>Angewandte Chemie - International Edition</i> , 2007, 46, 1419-1422.	14.8	395
188	Neutron Powder Diffraction Study of D ₂ Sorption in Cu ₃ (1,3,5-benzenetricarboxylate) ₂ . <i>Journal of the American Chemical Society</i> , 2006, 128, 15578-15579.	14.6	266
189	Quasielastic and inelastic neutron scattering study of the hydration of monoclinic and triclinic tricalcium silicate. <i>Chemical Physics</i> , 2006, 326, 381-389.	2.0	17
190	Inelastic neutron scattering from antiferromagnetically coupled nearest-neighbor spin pairs in Zn(Mn)O and Zn(Mn)Te. <i>Physica B: Condensed Matter</i> , 2006, 385-386, 388-390.	2.8	1
191	Hydrogen Storage in a Microporous Metal-Organic Framework with Exposed Mn ²⁺ Coordination Sites. <i>Journal of the American Chemical Society</i> , 2006, 128, 16876-16883.	14.6	1,090
192	Origin and removal of spurious background peaks in vibrational spectra measured by filter-analyzer neutron spectrometers. <i>Nuclear Instruments and Methods in Physics Research, Section A: Accelerators, Spectrometers, Detectors and Associated Equipment</i> , 2004, 517, 189-201.	1.6	52
193	Determination of hole-induced ferromagnetic exchange between nearest-neighbor Mn spins in p-type Zn _{1-x} Mn _x Te. <i>Journal of Magnetism and Magnetic Materials</i> , 2004, 272-276, E1545-E1546.	2.3	0
194	Determination of hole-induced ferromagnetic Mn-Mn exchange in p-type Zn _{1-x} Mn _x Te by inelastic neutron scattering. <i>Physica B: Condensed Matter</i> , 2004, 350, 36-39.	2.8	3
195	The Crystalline Enol of 1,3-Cyclohexanedione and Its Complex with Benzene: A Vibrational Spectra, Simulation of Structure and Dynamics and Evidence for Cooperative Hydrogen Bonding. <i>Journal of Physical Chemistry A</i> , 2004, 108, 7356-7363.	2.6	15
196	Investigation of the State of Water in Hydrating Layered Sodium Disilicate in Crystalline and Amorphous Forms by Quasi-Elastic Neutron Scattering. <i>Chemistry of Materials</i> , 2004, 16, 5042-5050.	7.1	14
197	Terahertz spectroscopy of short-chain polypeptides. <i>Chemical Physics Letters</i> , 2003, 375, 337-343.	2.7	145
198	Comparison of Boson Peaks in Polypropylenes. <i>Macromolecules</i> , 2003, 36, 520-521.	5.1	0

#	ARTICLE	IF	CITATIONS
199	Solid-State Ligand Dynamics in Interpenetrating Mn[N(CN) ₂] ₂ (Pyrazine): A Neutron Spectroscopy Study. Journal of the American Chemical Society, 2002, 124, 12600-12605.	14.6	19
200	Incoherent Quasi-elastic Neutron Scattering from Fructose in Water Solutions. Journal of Physical Chemistry B, 2001, 105, 7799-7804.	2.7	19
201	Quantum rotation of hydrogen in single-wall carbon nanotubes. Chemical Physics Letters, 2000, 329, 311-316.	2.7	129
202	A view of dynamics changes in the molten globule-native folding step by quasielastic neutron scattering. Edited by P. E. Wright. Journal of Molecular Biology, 2000, 301, 525-536.	4.3	58
203	Powder diffraction and inelastic neutron scattering studies of the Na ₂ RbC ₆₀ fulleride. Journal of Materials Chemistry, 2000, 10, 1443-1449.	6.7	3
204	Anomalous High Pressure Properties in Fullerene Superconductors. Molecular Crystals and Liquid Crystals, 2000, 340, 599-604.	0.3	2
205	Neutron diffraction study of the polymeric structure of C ₆₀ . Journal of Physics Condensed Matter, 1999, 11, 371-381.	1.9	11
206	Pressure dependence of superconductivity in the Na ₂ Rb _{0.5} Cs _{0.5} C ₆₀ fulleride. Physical Review B, 1999, 59, 4439-4444.	3.3	22
207	Rotational tunneling of ammonia in (NH ₃)K ₃ C ₆₀ . Journal of Chemical Physics, 1999, 111, 10969-10973.	3.1	1
208	Structural and Electronic Properties of the Noncubic Superconducting Fullerides A ₄ C ₆₀ (A = Ba, Sr). Physical Review Letters, 1999, 83, 2258-2261.	8.0	36
209	Superconductivity in Li _x CsC ₆₀ fullerides. Physical Review B, 1999, 59, R6628-R6630.	3.3	51
210	Pressure and Temperature Evolution of the Structure of the Superconducting Na ₂ CsC ₆₀ Fulleride. Journal of Solid State Chemistry, 1999, 145, 471-478.	3.0	23
211	Temperature and pressure dependence of orientational disorder and bonding in Li ₂ CsC ₆₀ . Solid State Sciences, 1999, 1, 157-163.	0.8	3
212	Band filling and width control in fullerides. Synthetic Metals, 1999, 103, 2462-2465.	4.1	0
213	Crystal Structure of the Higher Fullerene C ₈₄ . Chemistry of Materials, 1998, 10, 1742-1744.	7.1	32
214	Effects of Pressure on the Azafullerene (C ₅₉ N) ₂ Molecular Solid to 22 GPa. Journal of the American Chemical Society, 1996, 118, 8715-8716.	14.6	43
215	Interfullerene vibrations in the polymeric fulleride CsC ₆₀ . Chemical Communications, 1996, , 2465.	4.2	6
216	Geometric Tuning of Coordinatively Unsaturated Copper(I) Sites in Metal-Organic Frameworks for Ambient-Temperature Hydrogen Storage. Journal of the American Chemical Society, 0, , .	14.6	0

#	ARTICLE	IF	CITATIONS
217	Integrating crystallographic and computational approaches to carbon-capture materials for the mitigation of climate change. <i>Journal of Materials Chemistry A</i> , 0, , .	10.5	0